Calhoun: The NPS Institutional Archive

Faculty and Researcher Publications

2007

On the Source of Organic Acid Aerosol Layers above Clouds

Sorooshian, Armin

http://hdl.handle.net/10945/42258

On the Source of Organic Acid Aerosol Layers above Clouds

ARMIN SOROOSHIAN,[†] MIAO-LING LU,[†]
FRED J. BRECHTEL,[†,‡]
HAFLIDI JONSSON,[§]
GRAHAM FEINGOLD,[∥]
RICHARD C. FLAGAN,[†] AND
JOHN H. SEINFELD*[,†]

Departments of Environmental Science and Engineering and Chemical Engineering, California Institute of Technology, 1200 E. California Boulevard, Pasadena, California 91125, Brechtel Manufacturing Inc., 1789 Addison Way, Hayward, California 94544, Center for Interdisciplinary Remotely-Piloted Aircraft Studies, Naval Postgraduate School, 3200 Imjin Road, Hangar #507, Marina, California 93933, and Earth System Research Laboratory/Chemical Sciences Division, National Oceanic and Atmospheric Administration, 325 Broadway, Boulder, Colorado 80305

During the July 2005 Marine Stratus/Stratocumulus Experiment (MASE) and the August−September 2006 Gulf of Mexico Atmospheric Composition and Climate Study (GoMACCS), the Center for Interdisciplinary Remotely-Piloted Aircraft Studies (CIRPAS) Twin Otter probed aerosols and cumulus clouds in the eastern Pacific Ocean off the coast of northern California and in southeastern Texas, respectively. An on-board particle-into-liquid sampler (PILS) quantified inorganic and organic acid species with ≤5-min time resolution. Ubiquitous organic aerosol layers above cloud with enhanced organic acid levels were observed in both locations. The data suggest that aqueous-phase reactions to produce organic acids, mainly oxalic acid, followed by droplet evaporation is a source of elevated organic acid aerosol levels above cloud. Oxalic acid is observed to be produced more efficiently relative to sulfate as the cloud liquid water content increases, corresponding to larger and less acidic droplets. As derived from large eddy simulations of stratocumulus under the conditions of MASE, both Lagrangian trajectory analysis and diurnal cloudtop evolution provide evidence that a significant fraction of the aerosol mass concentration above cloud can be accounted for by evaporated droplet residual particles. Methanesulfonate data suggest that entrainment of free tropospheric aerosol can also be a source of organic acids above boundary layer clouds.

Introduction

Organic carbon (OC) is a major component of atmospheric particulate matter (*1−7*). Organic acids constitute a significant fraction of particulate organic carbon (*1, 8−11*). Dicarboxylic acids, the most abundant of which in the troposphere is oxalic acid [$(COOH)_2$], contributed as much as 50% to particulate organic aerosol mass in at least one study in central Japan (*8*). Primary emissions from fossil fuel combustion, biomass burning, and biogenic activity are sources of particulate oxalic acid (*12−14*); photooxidation of volatile organic compounds (VOCs), particularly aromatic hydrocarbons, followed by condensation onto preexisting aerosols is also a source (*15, 16*). Blando and Turpin (*17*) suggested that organic acids are likely particle-phase compounds formed by cloud and fog processing. Oxalic acid, which has also been shown to be formed by aqueous-phase chemistry in cloud droplets, remains in the aerosol phase after subsequent droplet evaporation (*18−28*). In the aqueous phase, oxalic acid is formed by oxidation of either glyoxylic acid or by the oxidative decay of malonic acid, which, in turn, is formed by the oxidation of higher order dicarboxylic acids (*18, 19, 21−28*). Sorooshian et al. (*21*) showed that the glyoxylic acid oxidation pathway is significantly more efficient at producing oxalic acid, as compared to malonic acid oxidation. Aqueous-phase intermediates to glyoxylic acid include glyoxal, methylglyoxal, glycolic acid, pyruvic acid, and acetic acid (*18, 19, 21−28*).

In July 2005, the Center for Interdisciplinary Remotely-Piloted Aircraft Studies (CIRPAS) Twin Otter (TO), based at Marina, CA, participated in the Marine Stratus/Stratocumulus Experiment (MASE), focused on probing aerosols and stratocumulus clouds over the eastern Pacific Ocean off the coast of northern California (*29*; http://www.cirpas.org). During August and September 2006, the CIRPAS TO also participated in the Gulf of Mexico Atmospheric Composition and Climate Study (*25*; GoMACCS; http://esrl.noaa.gov/csd/2006/), in which 22 flights were devoted largely to probing aerosol−cloud relationships over the Gulf of Mexico and the inland Houston area. In both MASE and GoMACCS, a ubiquitous layer of organic aerosol was found above cloud. These observations in the MASE experiment have been noted by Alexander et al. (*30*). At present, there is uncertainty as to what mechanism(s) can explain these observations. It should be noted that Heald et al. (*31, 32*) also observed a layer of enhanced organic aerosol levels, but in the free troposphere (FT), and argued that likely explanations include the formation of secondary organic aerosol (SOA) following the venting of insoluble VOCs to the FT and also cloud processing.

The goal of the present work is to evaluate, on the basis of the two field datasets, evidence and possible mechanisms for the existence of pervasive organic aerosol layers above clouds. We focus especially on organic acid levels in this work; particulate concentrations of organic acids and sulfate, and their ratios to each other, are compared above the boundary layer (BL) and below, inside, and above BL cumulus clouds. Results from large eddy simulations (LES) are used to provide support for a source of organic acid aerosols above cloud as residual particles from evaporated droplets.

Aircraft Measurements

The instrument payload on the TO aircraft is described elsewhere (*29*; http://www.cirpas.org). In both field experiments, two different inlets were employed for sampling clear air and clouds. A counterflow virtual impactor (CVI) inlet was used in cloud to isolate particles resulting from evaporation of cloud droplets (so-called residual particles). The transmission efficiency of the total aerosol inlet under standard flight conditions for particle diameters less than 3.5 μm is near unity (*33*). Submicrometer aerosol chemical composition measurements were carried out by a particle-into-liquid sampler (PILS, Brechtel Manufacturing Inc.) (*34*). In the PILS, submicrometer-sized ambient particles are grown into droplets sufficiently large to be collected by inertial

* Corresponding author phone: (626) 395-4635; fax: (626) 796-2591; e-mail: seinfeld@caltech.edu.
† California Institute of Technology.
‡ Brechtel Manufacturing Inc.
§ Center for Interdisciplinary Remotely-Piloted Aircraft Studies.
∥ National Oceanic and Atmospheric Administration.

Data Row 1: Oxalate ($\mu g/m^3$);[100*oxalate/organic acid mass] Data Row 2: Oxalate:SO_4^{2-} by mass Data Row 3: % samples with MSA detected;[MSA (ng/m^3)]	MASE	GoMACCS
FT averages		
	0.03±0.03	0.03±0.05[54±39]
	0.06±0.06	0.05±0.07
	28	13[3.0±7.4]
Above-cloud averages		
	0.07±0.04	0.11±0.11[87±17]
	0.09±0.07	0.12±0.12
	24	2[1.5±11.1]
In-cloud averages		
	NA	NA[81±24]
	0.08±0.06	0.08±0.08
	12	3
Below-cloud averages		
	0.05±0.03	0.08±0.10[69±30]
	0.05±0.05	0.02±0.03
	36	13[5.3±18.5]

Long-range transport — FT aerosol containing sulfate and organic acids

Top of BL

Above-cloud aerosol with sulfate and organic acids

Cloud — Droplets producing oxalic acid and sulfate — Interstitial aerosol

SO₂, VOCs — Below cloud aerosol containing sulfate and organic acids
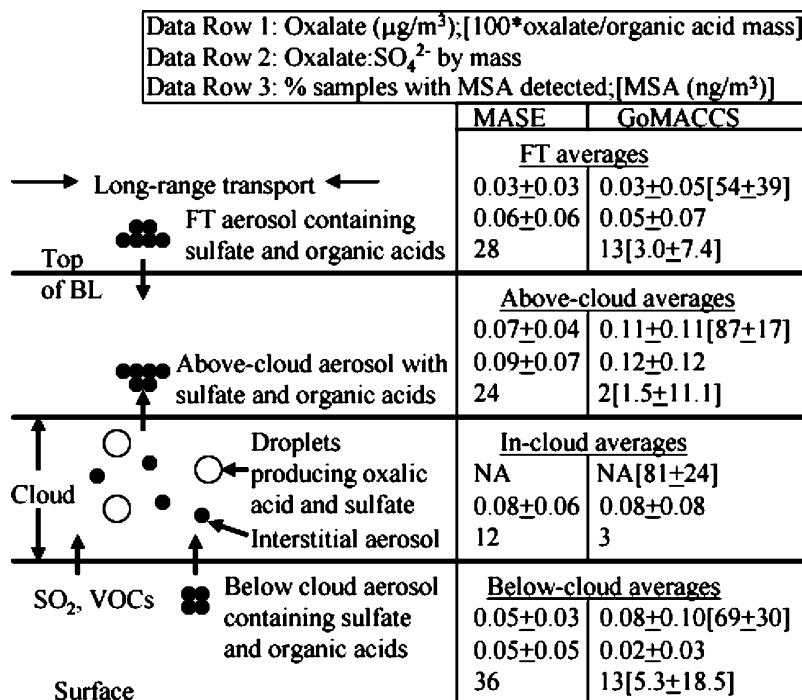
Surface

FIGURE 1. Schematic of physical processes leading to an organic acid aerosol layer above clouds. Average oxalate, sulfate, and methanesulfonate data are shown next to the respective region of the atmosphere where they were measured (below cloud, in cloud, above cloud, and the FT) for MASE and GoMACCS. During MASE, oxalate represented the entire organic acid mass (mass fraction is not shown) and absolute concentrations of MSA⁻ were not measured. In addition, only species ratios are reported for the in-cloud category since absolute concentrations were not measured (NA).

impaction, allowing subsequent chemical analysis by ion chromatography (IC, Dionex). A series of three denuders immediately downstream of the PILS inlet removes inorganic and organic gases that may bias aerosol measurements. Samples are deposited in vials held on a rotating carousel, where each vial contains material representing a period of time between 3.5 and 5 min of flight. IC analysis quantified the ambient air concentrations of water-soluble ions, including inorganic and organic acid ions.

The PILS-IC instrument uncertainty is calculated to be ±7% and the detection limit (calculated as the average concentration plus three standard deviations of the smallest detectable peak for each ion in the IC baseline noise and then converted to air-equivalent units) is <0.04 $\mu g/m^3$ for the inorganic ions (NH_4^+, SO_4^{2-}, and NO_3^-) and <0.01 $\mu g/m^3$ for the organic acid ions (dicarboxylic acids C_2–C_9, acetate, formate, pyruvate, glyoxylate, maleate, malate, methacrylate, benzoate, and methanesulfonate) pertinent to this study. Methanesulfonate (MSA⁻) was detected during MASE and GoMACCS, but was only quantified for GoMACCS flights because of uncertainties in its measurement during MASE; therefore, only the presence of MSA⁻ in MASE samples is reported, not its concentration. Oxalate is the only organic acid ion for which quantitative data are shown from MASE, as it was the only organic acid observed above detection limits.

The aircraft flight strategy consisted of probing either cloud fields (MASE and GoMACCS) or a single growing cumulus cloud (GoMACCS). The flight path generally comprised multiple level legs below cloud, at different altitudes in cloud, and above cloud. The cloud field legs were usually sufficiently long for at least two PILS samples to be collected, while individual samples collected during shorter single cloud profiling legs combined residual particles from up to three different altitude transects. Relative ratios of species in individual droplet residual particle samples are reported in this study, as opposed to absolute concentrations, to account

for the variable amount of time the aircraft spent in cloud when collecting a particular sample.

During MASE, stratocumulus cloud bases typically ranged between 100 and 400 m, with tops between 350 and 700 m. Cumulus cloud bases during GoMACCS ranged between 500 and 800 m, with tops between 800 and 3000 m. Typical stratocumulus liquid water content (LWC) values ranged between 0.1 and 0.5 g/m^3, with a maximum of 0.7 g/m^3, during MASE; cumulus LWC values between 0.1 and 1 g/m^3 were typically observed during GoMACCS, with a maximum of 2.1 g/m^3. Sounding profiles up to cloud bases indicate that the BL tended to be well-mixed during both field campaigns. An estimate of the in-cloud residence time of an air parcel in a well-mixed BL can be obtained from the cloud volume fraction of the BL (35), values of which for both field studies were usually between 20 and 50%. The volume fraction was calculated by dividing the average cloud depth observed during cloud field legs by the BL height; uncertainties in this calculation include the assumption that there was a continuous cloud deck of the same depth everywhere in the BL and that there was no deviation in cloud thickness. For GoMACCS, this likely represents an upper bound since cloud fractions were on the order of 10%. Organic acids constituted a significant portion of the above-cloud aerosol mass during both campaigns; on average, organic acid mass above cloud during MASE and GoMACCS was 0.07 ± 0.04 $\mu g/m^3$ (4.9 ± 3.6% of PILS mass) and 0.14 ± 0.14 $\mu g/m^3$ (6.5 ± 5.1% of PILS mass), respectively.

Sources of Oxalate above Cloud

Figure 1 is a schematic of processes that can lead to enhanced organic acid levels above cloud. Gases such as SO₂ and VOCs ascend into cloud and partition into droplets before participating in aqueous-phase chemistry to form SO_4^{2-} and organic species (such as oxalic acid), respectively (18–28). At the same time, ambient particles already containing SO_4^{2-} and organic acids are lofted into cloud. Above cloudtop,
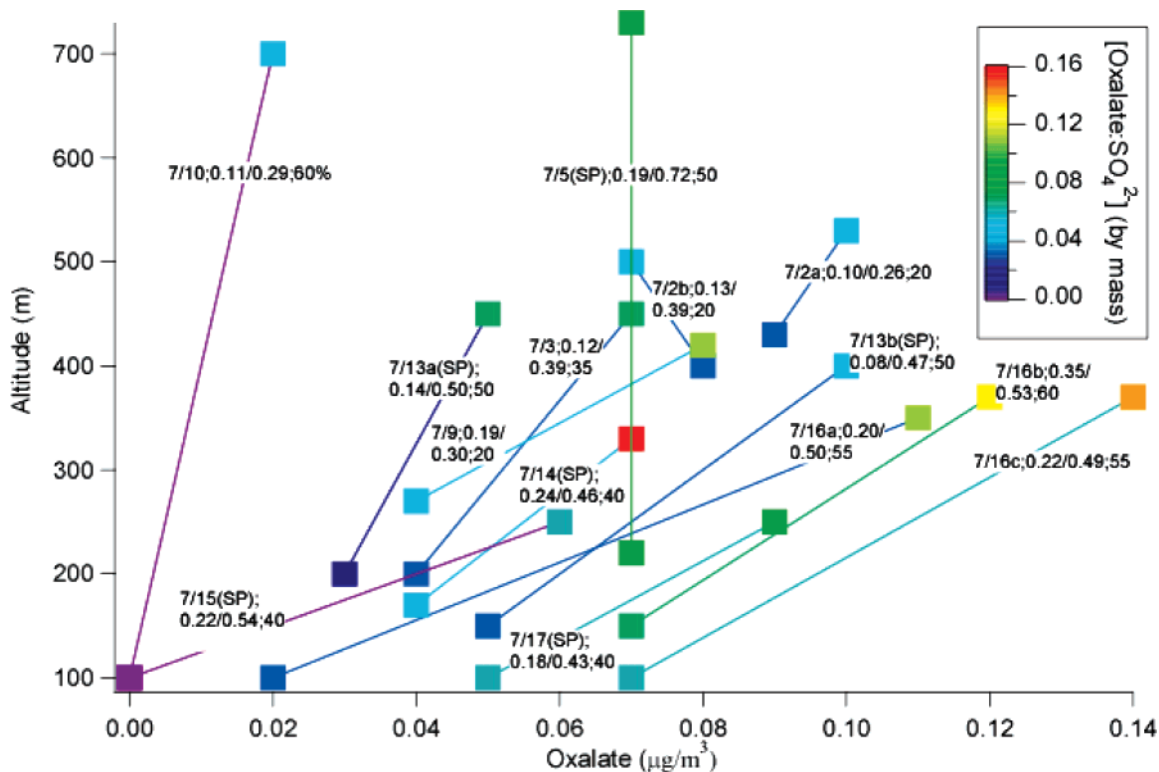
FIGURE 2. Particulate oxalate concentrations below and above 14 different cloud fields probed during MASE (lines connect below- and above-cloud measurements for individual cloud profiling events). The points are color coded with their respective oxalate:SO_4^{2-} mass ratios, which typically increased above cloud. The information in each text box corresponds to the following in order: date of flight; LWC average/maximum (g/m³); BL cloud volume fraction (%). Letters after the date signify multiple cloud fields studied during the same flight. "SP" corresponds to clouds influenced by ship plumes.

droplets evaporate leaving residual particles, which contain newly formed species such as sulfate and oxalic acid. Also, aerosol containing organic acids can be entrained into the BL from the FT. Although not discussed here, new particle formation can also occur above cloud (36).

Oxalate was consistently the dominant organic acid species measured in both field experiments; during Go-MACCS, for example, the largest contributor to above-cloud organic acids was oxalate, on average 87 ± 17% by mass (Figure 1). Less abundant species included acetate (7 ± 13%), formate (2 ± 8%), malonate (1 ± 6%), glutarate (1 ± 7%), MSA⁻ (1 ± 5%), succinate (0.5 ± 3%), and glyoxylate (0.5 ± 2%). During both MASE and GoMACCS, the oxalate concentration, on average, increased from below to above cloud by between 25 and 30%, then decreased above the BL to it lowest values in the FT (Figure 1).

Of 14 cloud field profiling events during MASE, oxalate concentration was higher above cloud as compared to below in 12 events (Figure 2). Sulfate was greater above cloud as compared to below in three of these 14 events (7/16a, 7/13b, 7/17), two of which were influenced by ship emissions; there was usually slightly less sulfate above cloud as compared to below. Situations in which the increase in NH_4^+:SO_4^{2-} from below to above cloud was largest tended to exhibit the greatest amount of oxalate growth as well (7/16a−c). The greatest increase in both oxalate concentration and the relative amount of oxalate to sulfate from below to above cloud was usually associated with higher in-cloud LWC values and larger BL cloud volume fractions. Four out of nine cloud events, in which at least four droplet residual samples were collected, exhibited a strong correlation between sulfate and oxalate ($R^2 > 0.5$); this is consistent with in-cloud production of oxalic acid (19, 21, 25, 26).

During GoMACCS, higher organic acid and oxalate mass concentrations were observed above cloud as compared to below in 13 and 16 out of 22 cloud profiling events, respectively (Figure 3). Only one event (8/23b), which was directly influenced by the plume from the W.A. Parish Power Plant, exhibited a higher sulfate concentration above cloud; sulfate was usually more abundant below cloud due to the high background levels at lower altitudes from local SO_2 sources. When BL cloud volume fractions exceeded 55% in GoMACCS, the contribution of oxalate to organic acid mass in aerosol below and above cloud always exceeded 85% and 90%, respectively; these values were lower when the BL cloud volume fraction was smaller, presumably because the cloud droplet medium in which organic acids are converted to oxalic acid was less abundant. Similar to MASE, oxalate was well-correlated with sulfate in cloud ($R^2 > 0.5$ in 14 out of the 22 events). It should be noted that in cloud events from both field campaigns where oxalate increased from below to above cloud, the increases were significant beyond the PILS-IC measurement uncertainty.

During strong GoMACCS pollution events (>8000 particles/cm³ below cloud) the contribution of oxalate to the total organic acid mass increased from below to above cloud even though the total organic acid mass itself decreased (8/23b, 9/2b). Under more polluted conditions, photooxidation of primary VOCs may have led to lower volatility organic acids that could have partitioned into below-cloud aerosols. It is hypothesized that subsequent cloud processing increased the oxalate mass above these polluted clouds, with simultaneous depletion of the other organic acids by deposition, reaction to form volatile organic side-products, or further oxidation to produce oxalic acid.

Physical Processes at the Cloudtop Interface (Large Eddy Simulations)

To assess the likelihood of there being evaporated droplet residual particles above cloud, we report on LES results for
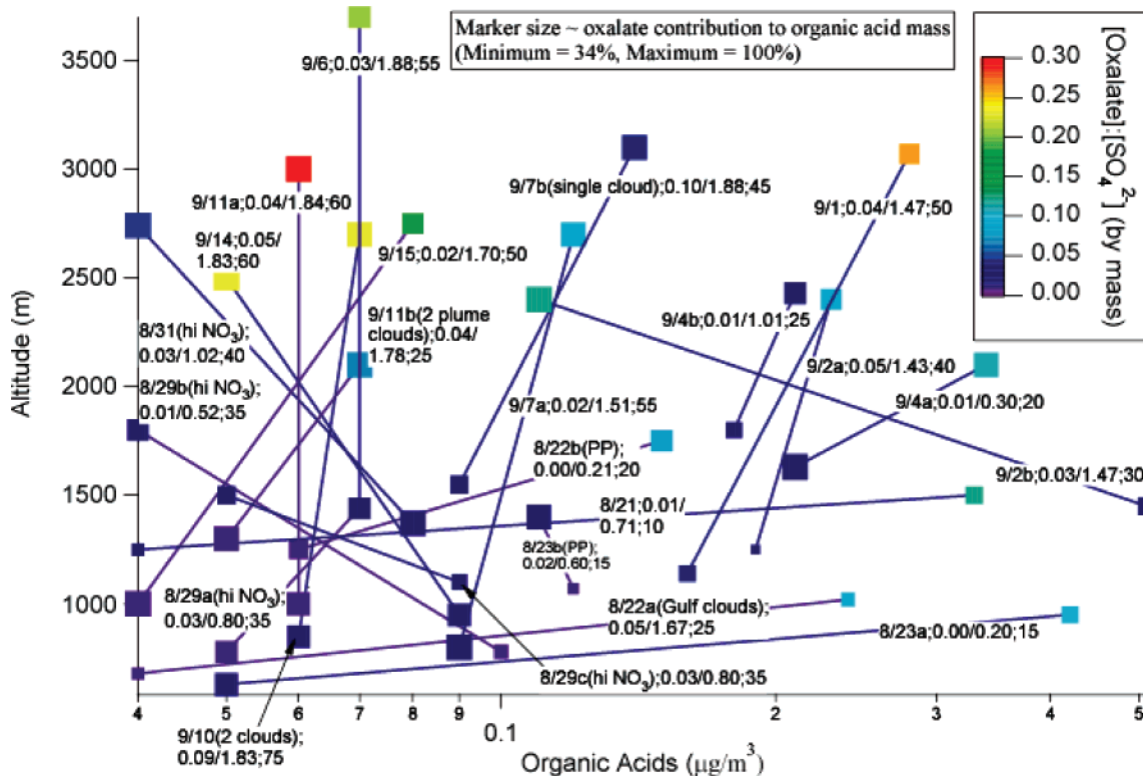
FIGURE 3. Particulate organic acid concentrations below and above 22 different cloud systems probed during GoMACCS (lines connect below- and above-cloud measurements for individual cloud profiling events). The points are color coded with their respective oxalate:SO_4^{2-} mass ratios, which typically increased above cloud. Larger marker sizes, usually above cloud, also denote that oxalate contributed relatively more to the total organic acid mass. The information in each text box corresponds to the following in order: date of flight; LWC average/maximum (g/m³); BL cloud volume fraction (%). Letters after the date signify multiple cloud fields studied during the same flight. "PP" corresponds to clouds influenced by the Parish Plant plume.

the stratocumulus cloud observed July 5, 2005, which was influenced by ship emissions. For vertical resolution, we use $\Delta z = 5$ m near the cloudtop interface ($z = 630-730$ m); outside that range, a resolution of 15 m is employed, giving a total of 94 vertical grid cells. The horizontal resolution is 55 m with 60 grid cells in each horizontal direction. Periodic boundary conditions are specified (*37*). The sea surface temperature is taken to be 287 K. The large scale divergence estimated from the National Centers for Environmental Prediction (NCEP) reanalysis is set at 10^{-5}/s. The initial wind field is assumed to be constant with $u = 5.75$ m/s and $v = -9.96$ m/s, as derived from the aircraft measurements. The initial sounding profiles are based on the smoothed vertical profiles of potential temperature and total liquid water mixing ratio sampled by the aircraft. The model is spun up at 4 a.m. local time with random noise on temperature over the initially assumed well-mixed sounding profile. The model used is the LES version of RAMS coupled with bin microphysics, a detailed description of which is given by Lu and Seinfeld (*37*).

The dry aerosol size distribution obtained by the differential mobility analyzer in the sub-cloud region (~227 m) is fitted with a trimodal log-normal distribution: r_g [nm] = (56, 65, 175), σ_g = (1.24, 2.43, 1.31), and N [cm^{-3}] = (140, 513, 81). Based on aircraft measurements, the simulated CCN is largely ammonium bisulfate with dry density of 1.79 g/cm³ and soluble fraction of 1. Organic carbon is not considered as an aerosol component in the LES simulations.

Lagrangian air parcel trajectories from the LES simulations are derived following the methodology of Stevens et al. (*38*). The parcels are released at 10 a.m. local time and tracked for 3 h; 3600 parcels are released at each altitude. The integration time interval for parcel trajectories is 10 s. Parcels initialized just below cloudtop have the highest probability of ascending

above cloud (Figure 4A−C); at least 10% of cloud parcels that originate within the 10 m layer below cloudtop can ascend above cloud (Table 1). These above-cloud parcels can be recycled back into cloud or remain above cloud. Cloudtop residence times of simulated trajectories in nonprecipitating stratocumulus have been shown to be on the order of 10 min or longer (*38*); a significant portion of droplets near cloudtop, as represented by trajectories in the present simulations, are likely to undergo evaporation once they are out of cloud.

Stratocumulus clouds typically exhibit a clear diurnal evolution in cloud top and base (*37, 39*), and the cloud layer is thinner during daytime as compared to nighttime. LES results in Figure 4D show that the simulated cloudtop drops by about 15 m from 8 to 10 a.m. Extrapolating these results to the actual measurements suggests that the thin layer above cloud sampled by the aircraft possibly contained droplet residual particles from evaporated cloudtops during the day. Moreover, modeling studies of marine stratocumulus clouds have shown that cloudtops are not the limit of mixing of BL air and that turbulence and mixing tend to exist up to tens of meters above cloud (*40, 41*). Hegg et al. (*42*) reported measurements directly above stratocumulus off the coast of California, as in the present experiment; their measurements also indicate that cloud-processed aerosol detraining from the marine cloud layer were being sampled. In summary, both Lagrangian trajectory analysis and diurnal cloud top evolution provide evidence that a significant fraction of aerosol particles above cloud are likely residual particles from evaporated cloud droplets. Both mechanisms work concomitantly and continuously during the day, as the resultant residual particle layer thickens. This conceptual model provides support for physical mechanisms leading to a residual organic acid aerosol layer above clouds.
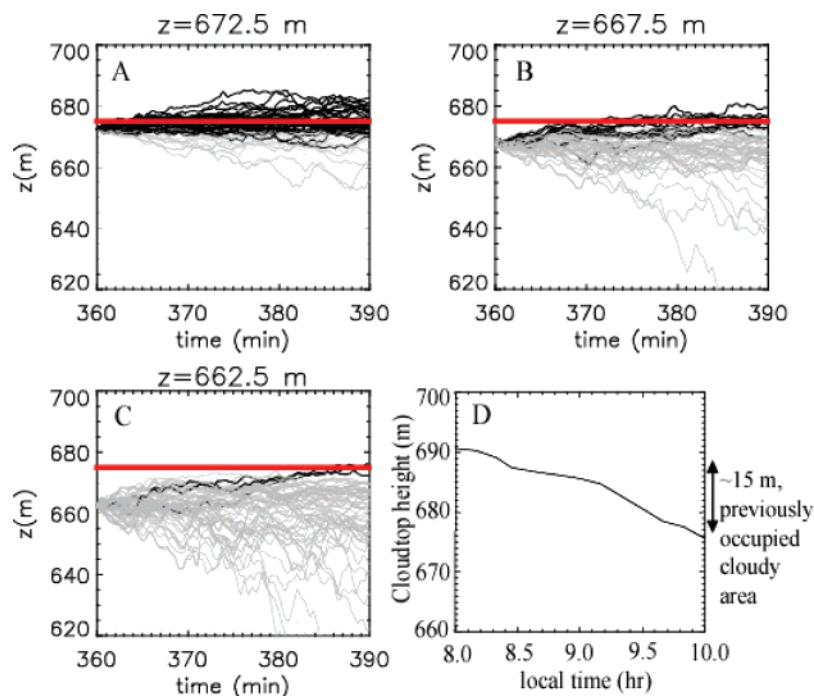
FIGURE 4. (A—C) Example of the temporal evolution of trajectories from a 2D slice of the 3D LES simulation. Trajectories are initialized at various altitudes (z) near cloudtop. Trajectories that always stay inside cloud are shown as gray lines; those that penetrate above cloud at least once are represented by black lines. The thick red horizontal line marks the cloudtop (675 m). (D) Temporal evolution of cloudtop from the LES simulation of the stratocumulus cloud observed July 5, 2005, which was influenced by ship emissions (corresponds to 7/5 in Figure 2). Detailed discussion of this cloud can be found in Lu et al. (*29*).

TABLE 1. Summary of Lagrangian Trajectory Results

initial trajectory altitude (m) (cloudtop = 675 m)	fraction of trajectories penetrating above cloudtop at least once (%)	mean cloud droplet number concentration (no./cm³)
672.5	56	159 ± 67
667.5	13	303 ± 112
662.5	4	284 ± 185

We utilize the results from the trajectory analysis to assess the amount of organic acid mass measured above cloud. Using results from Table 1, specifically that 56% of 159 droplets/cm³ ascend above cloudtop, and assuming that residual particles from these evaporated droplets have diameters of 150 nm, the density of ammonium bisulfate (1.79 g/cm³), and an organic acid mass fraction of 5% (based on measurements), the particulate organic acid concentration calculated (~0.01 μg/m³) is less than those measured. An increase in any of the input variables will increase this value, and this calculation still does not account for the thickening of the residual particle layer during the day. Assuming that all the aerosol above cloud consisted of evaporated droplets at 1000 particles/cm³, 0.16 μg/m³ of organic acids is predicted to be present, which approaches the highest measurement made above cloud during MASE (Figure 2: 7/16c = 0.14 μg/m³). The more convective clouds encountered during Go-MACCS, as compared to the stratocumulus clouds in MASE, would have been more effective at pumping cloud-processed aerosol above their tops. Vigorous mixing and transient cloud evolution (clouds grow and dissipate rapidly during the day) during GoMACCS likely contributed to the observed organic acid aerosol layer above cloud; during above-cloud legs, the aircraft was frequently sampling in areas that were recently occupied by the top portions of a cloud that evaporated.

Oxalic Acid Chemistry

Detection of aqueous-phase intermediates to oxalic acid in several cloud events provides evidence for a cloud processing mechanism. Glyoxylate was detected in droplet residual particles in six GoMACCS cloud events. Typically, the glyoxylate concentration in total aerosol samples was an order of magnitude lower than that of oxalate, with glyoxylate peaking at 0.03 μg/m³. Acetic acid, an aqueous precursor to glyoxylic acid, was measured during the same six events as well. The six cloud events were marked by higher LWC values as compared to others, which may explain why aqueous oxalic acid precursors reached measurable concentrations. Higher LWC values increase partitioning of gases (including organic precursors to oxalic acid) into droplets, which promotes enhanced production of oxalic acid from oxidation of intermediates such as glyoxylic and acetic acids.

It has been shown that glyoxylic acid produces oxalic acid more efficiently at higher droplet pH values, because the rate constant of the oxidation of glyoxylic acid is an order of magnitude lower than that of its anion, glyoxylate (*43*). Also, effective Henry's Law coefficients are a function of pH; higher acidity reduces droplet uptake efficiency for aqueous-phase precursors to oxalic acid. Similarly, the solubility of sulfate precursors and the aqueous oxidation of these precursors both have pH dependence. However, the production rate of oxalic acid is greater than that of sulfate at pH levels expected in cloud droplets; the Henry's Law coefficients for oxalic acid VOC precursors (for example, glyoxal = 3×10^5 M/atm; acetic acid = 5500 M/atm, pyruvic acid = 3.11×10^5 M/atm; glycolic and glyoxylic acids = 9000 M/atm) exceed that of SO₂ (1.24 M/atm) (*1*, *44*). In addition, at higher droplet pH conditions, the reaction rate constant for oxalic acid production from OH oxidation of glyoxylate, 2.9×10^9 M^{-1} s^{-1} (OH oxidation of glyoxylic acid = 3.6×10^8 M^{-1} s^{-1}), exceeds that of sulfate-producing reactions (SO₂ + O₃ = 2.4×10^4 M^{-1} s^{-1}; HSO₃⁻ + O₃ = 3.7×10^5 M^{-1} s^{-1}; SO₃²⁻ + O₃ = 1.5×10^9 M^{-1} s^{-1}; H₂O₂ + HSO₃⁻ + H⁺ = 7.2×10^7 M^{-2} s^{-1}) (*43*, *44*).
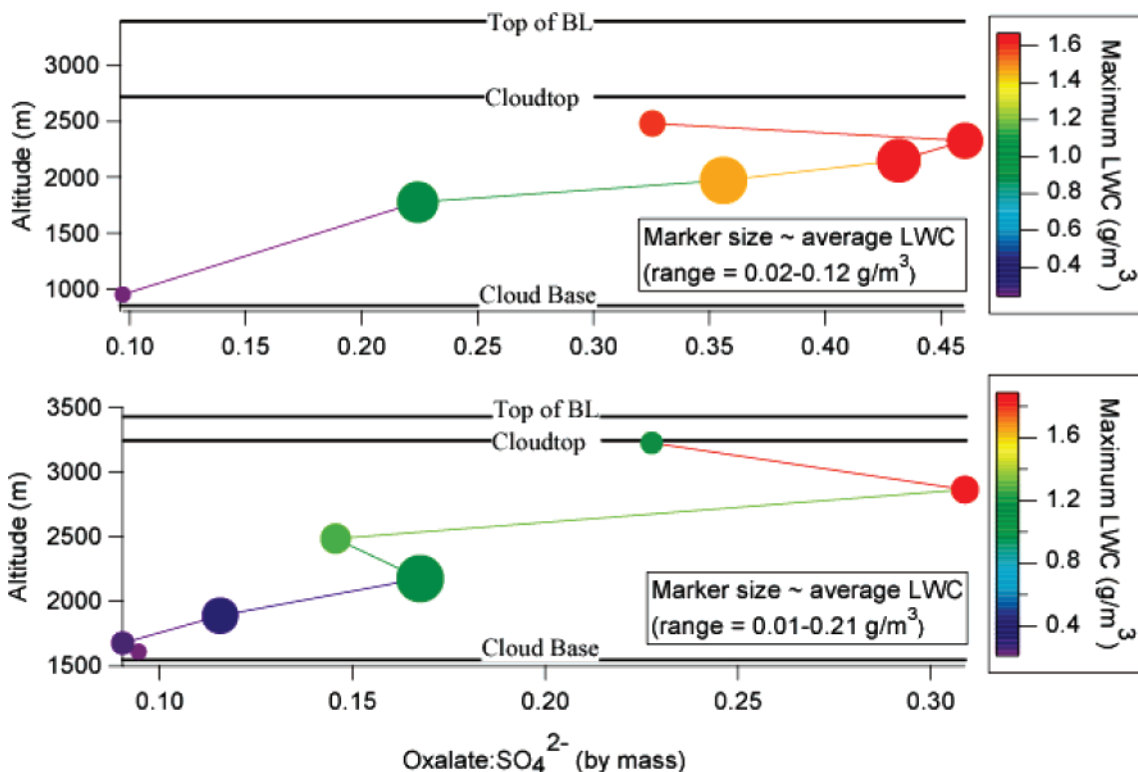
FIGURE 5. Droplet residual particle data from two different GoMACCS cloud profiling events. (Top) The TO probed two adjacent cumuli (corresponds to 9/10 in Figure 3); (Bottom) the TO probed one cumulus cloud (corresponds to 9/7b in Figure 3). The mass ratio of oxalate to sulfate usually increased with increasing LWC.

GoMACCS cloud data are consistent with a role of acidity in in-cloud processes. The oxalate:SO_4^{2-} ratio increased when ascending from below to above cloud in all MASE and GoMACCS cloud events, before decreasing above the BL. The below- to above-cloud ratio of oxalate to sulfate exhibited the largest increase when BL cloud volume fractions exceeded 55%; these cases also included cloud fields with some of the highest LWC values. During a single cloud profiling event (Figure 5: bottom), seven residual particle samples were collected with ascending altitude in a growing cumulus cloud, and the oxalate:SO_4^{2-} ratio increased in strong correlation with the maximum LWC amount. The greatest increases in the oxalate:SO_4^{2-} ratio occurred in the fourth and sixth sample when the greatest increases in the maximum LWC occurred. Cloud LWC increased with altitude, but decreased near cloudtop due to entrainment drying. In another cloud profiling event where two adjacent growing cumulus clouds were probed (Figure 5: top), the same trends were observed for six residual particle samples collected. The oxalate:SO_4^{2-} ratio grew with altitude as the maximum LWC increased, with the sharpest increases occurring with the maximum LWC increase. The cumuli in the two events were almost the same depth and exhibited similar oxalate:SO_4^{2-} mass ratios with altitude (0.10−0.40); the highest ratios were observed in the top half of the clouds. Observations from these cloud profiling events show that higher altitudes in cloud have increased LWC (with the exception of near the top due to entrainment drying) and as a result, higher droplet pH; the rate of oxalic acid production is enhanced relative to sulfate with increasing LWC in cloud. Also, higher oxalic acid concentrations relative to sulfate in the upper levels of clouds are a consequence of multistep aqueous-phase oxalic acid production (several subsequent oxidation steps are necessary before oxalic acid is formed from VOC precursors, whereas fewer steps are required for sulfate production; *18−28*), which is facilitated by more time in cloud. The oxalate:SO_4^{2-} ratio showed no increasing trend with altitude on clear days; most

of the higher clear air ratios were observed during flights when the plane was performing a spiral ascent or descent in an area near clouds. These results offer an explanation of high ratios of oxalate to sulfate above cloud.

Of 22 flights during GoMACCS, only two showed consistent particulate nitrate levels above 0.5 $\mu g/m^3$ in the BL. In these, the sampled particles exhibited NH_4^+:SO_4^{2-} molar ratios above two, indicating that there was sufficient NH_3 to neutralize SO_4^{2-}, thereby allowing HNO_3 to partition into the particle phase, forming NO_3^-. Four total cloud profiling events were carried out during these two flights (Figure 3: 8/29a−c, 8/31) in the high-nitrate area. Three of these events exhibited lower particulate oxalate and organic acid concentrations above cloud as compared to below. The oxalate:SO_4^{2-} ratio showed either no change or only a small increase from below to above cloud. In the presence of high HNO_3 levels and relatively lower LWC values, the droplets are more acidic, presumably suppressing organic acid formation. That the in-cloud production rate of oxalate seemed to be reduced during these cloud events suggests again that FT entrainment is not the dominant source of above-cloud oxalate levels.

Methanesulfonate

Methanesulfonate data from both campaigns show that the aerosol both above the BL and below clouds can be a source for this species above clouds. Methanesulfonic acid is formed by dimethylsulfide (DMS) oxidation by free radicals such as OH, where DMS is excreted by phytoplankton in seawater (*45*). Data from MASE and GoMACCS show that, on average, oxalate increased in concentration with altitude from below to above cloud; MSA^- exhibited the opposite behavior (Figure 1). MSA^- was most frequently detected below cloud; its frequency of detection decreased with altitude until eventually increasing above cloud. Since the occurrence of MSA^- was not observed to be enhanced in cloud, its source above cloud is more likely to be from above the BL. Most of the

GoMACCS MSA⁻ measurements occurred over the Gulf of Mexico; although not reflected in the average concentrations in Figure 1, comparable levels of MSA⁻ were measured above cloud and in the FT over the Gulf (0.02−0.05 μg/m³), with a decrease observed in cloud.

Five-day back-trajectories computed from the NOAA HYSPLIT model (46) for MASE indicate that the air tended to originate from areas over the Pacific Ocean farther north up the coast of the United States and from farther west over the ocean. Five-day back-trajectories indicate that air parcels in the GoMACCS flights with MSA⁻ detected originated farther southeast over the Gulf of Mexico. Vertical transport from the marine BL injects MSA⁻ or its precursors, such as DMS, into the lower FT. It is hypothesized that the MASE marine BL, which exhibited continuous decks of stratocumulus clouds, was more effective at entraining MSA⁻ enriched aerosol above clouds. The data indicate that the FT is a source of above-cloud MSA⁻ in both regions studied, and organic acids other than MSA⁻ may also be contained within these entraining aerosol particles.

Acknowledgments

Literature Cited

(1) Saxena, P.; Hildemann, L. M. Water-soluble organics in atmospheric particles: A critical review of the literature and application of thermodynamics to identify candidate compounds. *J. Atmos. Chem.* **1996**, *24*, 57−109.

(2) Kanakidou, M.; Seinfeld, J. H.; Pandis, S. N.; Barnes, I.; Dentener, F. J.; Facchini, M. C.; Van Dingenen, R.; Ervens, B.; Nenes, A.; Nielsen, C. J.; Swietlicki, E.; Putaud, J. P.; Balkanski, Y.; Fuzzi, S.; Horth, J.; Moortgat, G. K.; Winterhalter, R.; Myhre, C. E. L.; Tsigaridis, K.; Vignati, E.; Stephanou, E. G.; Wilson, J. Organic aerosol and global climate modelling: a review. *Atmos. Chem. Phys.* **2005**, *5*, 1053−1123.

(3) Lim, H. J.; Turpin, B. J. Origins of primary and secondary organic aerosol in Atlanta: Results of time-resolved measurements during the Atlanta supersite experiment. *Environ. Sci. Technol.* **2002**, *36*, 4489−4496.

(4) Balasubramanian, R.; Qian, W. B.; Decesari, S.; Facchini, M. C.; Fuzzi, S. Comprehensive characterization of PM2.5 aerosols in Singapore. *J. Geophys. Res.* **2003**, *108*, D16, 4523, doi:10.1029/2002JD002517.

(5) Putaud, J. P.; Raes, F.; Van Dingenen, R.; Bruggemann, E.; Facchini, M. C.; Decesari, S.; Fuzzi, S.; Gehrig, R.; Huglin, C.; Laj, P.; Lorbeer, G.; Maenhaut, W.; Mihalopoulos, N.; Mulller, K.; Querol, X.; Rodriguez, S.; Schneider, J.; Spindler, G.; ten Brink, H.; Torseth, K.; Wiedensohler, A. European aerosol phenomenology-2: chemical characteristics of particulate matter at kerbside, urban, rural and background sites in Europe. *Atmos. Environ.* **2004**, *38*, 2579−2595.

(6) Russell, M.; Allen, D. T.; Collins, D. R.; Fraser, M. P. Daily, seasonal, and spatial trends in PM2.5 mass and composition in Southeast Texas. *Aerosol Sci. Technol.* **2004**, *38*, 14−26.

(7) Murphy, D. M.; Cziczo, D. J.; Froyd, K. D.; Hudson, P. K.; Matthew, B. M.; Middlebrook, A. M.; Peltier, R. E.; Sullivan, A.; Thomson, D. S.; Weber, R. J. Single-particle mass spectrometry of tropospheric aerosol particles. *J. Geophys. Res.* **2006**, *111*, D23S32, doi:10.1029/2006JD007340.

(8) Satsumabayashi, H.; Kurita, H.; Yokouchi, Y.; Ueda, H. Photochemical formation of particulate dicarboxylic-acids under long-range transport in central Japan. *Atmos. Environ.* **1990**, *24*, 1443−1450.

(9) Kavouras, I. G.; Mihalopoulos, N.; Stephanou, E. G. Formation of atmospheric particles from organic acids produced by forests. *Nature* **1998**, *395*, 683−686.

(10) Kawamura, K.; Sakaguchi, F. Molecular distributions of water soluble dicarboxylic acids in marine aerosols over the Pacific Ocean including tropics. *J. Geophys. Res.* **1999**, *104*, D3, 3501−3509.

(11) Raman, R. S.; Hopke, P. K. An ion chromatographic analysis of water-soluble, short-chain organic acids in ambient particulate matter. *Int. J. Environ. Anal. Chem.* **2006**, *86*, 767−777.

(12) Kawamura, K.; Kaplan, I. R. Motor exhaust emissions as a primary source for dicarboxylic acids in Los Angeles ambient air. *Environ. Sci. Technol.* **1987**, *21*, 105−110.

(13) Narukawa, M.; Kawamura, K.; Takeuchi, N.; Nakajima, T. Distribution of dicarboxylic acids and carbon isotopic compositions in aerosols from 1997 Indonesian forest fires. *Geophys. Res. Lett.* **1999**, *26*, 3101−3104.

(14) Yamasoe, M. A.; Artaxo, P.; Miguel, A. H.; Allen, A. G. Chemical composition of aerosol particles from direct emissions of vegetation fires in the Amazon Basin: water-soluble species and trace elements. *Atmos. Environ.* **2000**, *34*, 1641−1653.

(15) Kleindienst, T. E.; Smith, D. F.; Li, W.; Edney, E. O.; Driscoll, D. J.; Speer, R. E.; Weathers, W. S. Secondary organic aerosol formation from the oxidation of aromatic hydrocarbons in the presence of dry submicron ammonium sulfate aerosol. *Atmos. Environ.* **1999**, *33*, 3669−3681.

(16) Kalberer, M.; Yu, J.; Cocker, D. R.; Flagan, R. C.; Seinfeld, J. H. Aerosol formation in the cyclohexene-ozone system. *Environ. Sci. Technol.* **2000**, *34*, 4894−4901.

(17) Blando, J. D.; Turpin, B. J. Secondary organic aerosol formation in cloud and fog droplets: a literature evaluation of plausibility. *Atmos. Environ.* **2000**, *34*, 1623−1632.

(18) Warneck, P. In-cloud chemistry opens pathway to the formation of oxalic acid in the marine atmosphere. *Atmos. Environ.* **2003**, *37*, 2423−2427.

(19) Crahan, K. K.; Hegg, D.; Covert, D. S.; Jonsson, H. An exploration of aqueous oxalic acid production in the coastal marine atmosphere. *Atmos. Environ.* **2004**, *38*, 3757−3764.

(20) Gelencser, A.; Varga, Z. Evaluation of the atmospheric significance of multiphase reactions in atmospheric secondary organic aerosol formation. *Atmos. Chem. Phys.* **2005**, *5*, 2823−2831.

(21) Sorooshian, A.; Varutbangkul, V.; Brechtel, F. J.; Ervens, B.; Feingold, G.; Bahreini, R.; Murphy, S. M.; Holloway, J. S.; Atlas, E. L.; Buzorius, G.; Jonsson, H.; Flagan, R. C.; Seinfeld, J. H. Oxalic acid in clear and cloudy atmospheres: Analysis of data from International Consortium for Atmospheric Research on Transport and Transformation 2004. *J. Geophys. Res.* **2006**, *111*, D23S45, doi:10.1029/2005JD006880.

(22) Ervens, B.; Feingold, G.; Frost, G. J.; Kreidenweis, S. M. A modeling study of aqueous production of dicarboxylic acids: 1. Chemical pathways and speciated organic mass production. *J. Geophys. Res.* **2004**, *109*, D15205, doi:10.1029/2003JD004387.

(23) Lim, H. J.; Carlton, A. G.; Turpin, B. J. Isoprene forms secondary organic aerosol through cloud processing: Model simulations. *Environ. Sci. Technol.* **2005**, *39*, 4441−4446.

(24) Carlton, A. G.; Turpin, B. J.; Lim, H. J.; Altieri, K. E.; Seitzinger, S. Link between isoprene and secondary organic aerosol (SOA): Pyruvic acid oxidation yields low volatility organic acids in clouds. *Geophys. Res. Lett.* **2006**, *33*, L06822, doi:10.1029/2005GL025374.

(25) Sorooshian, A.; Ng, N. L.; Chan, A. W. H.; Feingold, G.; Flagan, R. C.; Seinfeld, J. H. Particulate organic acids and overall water-soluble aerosol composition measurements from the 2006 Gulf of Mexico Atmospheric Composition and Climate Study (Go-MACCS). *J. Geophys. Res.* **2007**, doi:10.1029/2007JD008537, in press.

(26) Yu, J. Z.; Huang, S. F.; Xu, J. H.; Hu, M. When aerosol sulfate goes up, so does oxalate: Implication for the formation mechanisms of oxalate. *Environ. Sci. Technol.* **2005**, *39*, 128−133.

(27) Altieri, K. E.; Carlton, A. G.; Lim, H. J.; Turpin, B. J.; Seitzinger, S. P. Evidence for oligomer formation in clouds: Reactions of isoprene oxidation products. *Environ. Sci. Technol.* **2006**, *40*, 4956−4960.

(28) Carlton, A. G.; Turpin, B. J.; Altieri, K. E.; Seitzinger, S.; Reff, A.; Lim, H. J.; Ervens, B. Atmospheric oxalic acid and SOA production from glyoxal: results of aqueous photooxidation experiments. *Atmos. Environ.* **2007**, in press.

(29) Lu, M.-L.; Conant, W. C.; Jonsson, H.; Varutbangkul, V.; Flagan, R. C.; Seinfeld, J. H. The Marine Stratus/Stratocumulus Experiment (MASE): Aerosol-cloud relationships in marine stratocumulus. *J. Geophys. Res.* **2007**, doi:10.1029:/2006JD007985, in press.

(30) Alexander, M.; Hubbe, J.; Lee, Y.; Daum, P.; Senum, G.; Wang, J.; Flagan, R. C.; Varutbangkul, V.; Murphy, S. M.; Rissman, T. A.; Sorooshian, A.; Seinfeld, J. H.; Hudson, J.; Jayne, J. Observation of persistent layer of enhanced organic aerosol concentrations above cloudtops off the Northern California Coast; Seventh

International Aerosol Conference, American Association for Aerosol Research, St. Paul, MN, September 10−15, 2006.

(31) Heald, C. L.; Jacob, D. J.; Park, R. J.; Russell, L. M.; Huebert, B. J.; Seinfeld, J. H.; Liao, H.; Weber, R. J. A large organic aerosol source in the free troposphere missing from current models. *Geophys. Res. Lett.* **2005**, *32*, L18809, doi:10.1029/2005GL023831.

(32) Heald, C. L.; Jacob, D. J.; Turquety, S.; Hudman, R. C.; Weber, R. J.; Sullivan, A. P.; Peltier, R. E.; Atlas, E. L.; de Gouw, J. A.; Warneke, C.; Holloway, J. S.; Neuman, J. A.; Flocke, F. M.; Seinfeld, J. H. Concentrations and sources of organic carbon aerosols in the free troposphere over North America. *J. Geophys. Res.* **2006**, *111*, D23S47, doi:10.1029/2006JD007705.

(33) Hegg, D. A.; Covert, D. S.; Covert, P. A.; Jonsson, H. Determination of the efficiency of an aircraft aerosol inlet. *Aerosol Sci. Technol.* **2005**, *39*, 966− 971.

(34) Sorooshian, A.; Brechtel, F. J.; Ma, Y. L.; Weber, R. J.; Corless, A.; Flagan, R. C.; Seinfeld, J. H. Modeling and characterization of a particle-into-liquid sampler (PILS). *Aerosol Sci. Technol.* **2006**, *40*, 396−409.

(35) Feingold, G.; Kreidenweis, S. M.; Zhang, Y. Stratocumulus processing of gases and cloud condensation nuclei: 1. Trajectory ensemble model. *J. Geophys. Res.* **1998**, *103*, D16, 19527−19542.

(36) Hegg, D. A.; Radke, L. F.; Hobbs, P. V. Particle-production associated with marine clouds. *J. Geophys. Res.* **1990**, *95*, D9, 13917−13926.

(37) Lu, M.-L.; Seinfeld, J. H. Study of the aerosol indirect effect by large-eddy simulation of marine stratocumulus. *J. Atmos. Sci.* **2005**, *62*, 3909−3932.

(38) Stevens, B.; Feingold, G.; Cotton, W. R.; Walko, R. L. Elements of the microphysical structure of numerically simulated non-precipitating stratocumulus. *J. Atmos. Sci.* **1996**, *53*, 980−1006.

(39) Duynkerke, P. G.; de Roode, S. R.; van Zanten, M. C.; Calvo, J.; Cuxart, J.; Cheinet, S.; Chlond, A.; Grenier, H.; Jonker, P. J.; Kohler, M.; Lenderink, G.; Lewellen, D.; Lappen, C. L.; Lock, A. P.; Moeng, C. H.; Muller, F.; Olmeda, D.; Piriou, J. M.; Sanchez, E.; Sednev, I. Observations and numerical simulations of the diurnal cycle of the EUROCS stratocumulus case. *Q. J. R. Meteor. Soc.* **2004**, *130*, 3269−3296.

(40) Moeng, C. H.; Stevens, B.; Sullivan, P. P. Where is the interface of the stratocumulus-topped PBL?. *J. Atmos. Sci.* **2005**, *62*, 2626−2631.

(41) Lenschow, D. H.; Zhou, M. Y.; Zeng, X. B.; Chen, L. S.; Xu, X. D. Measurements of fine-scale structure at the top of Marine Stratocumulus. *Bound.-Lay. Meteorol.* **2000**, *97*, 331−357.

(42) Hegg, D. A.; Covert, D. S.; Jonsson, H.; Khelif, D.; Friehe, C. A. Observations of the impact of cloud processing on aerosol light-scattering efficiency. *Tellus B* **2004**, *56*, 285−293.

(43) Ervens, B.; Gligorovski, S.; Herrmann, H. Temperature-dependent rate constants for hydroxyl radical reactions with organic compounds in aqueous solutions. *Phys. Chem. Chem. Phys.* **2003**, *5*, 1811−1824.

(44) Ervens, B.; George, C.; Williams, J. E.; Buxton, G. V.; Salmon, G. A.; Bydder, M.; Wilkinson, F.; Dentener, F.; Mirabel, P.; Wolke, R.; Herrmann, H. CAPRAM 2.4 (MODAC mechanism): An extended and condensed tropospheric aqueous phase mechanism and its application. *J. Geophys. Res.* **2003**, *108*, D14, 4426, doi:10.1029/2002JD002202.

(45) Charlson, R. J.; Lovelock, J. E.; Andreae, M. O.; Warren, S. G. Oceanic phytoplankton, atmospheric sulphur, cloud albedo and climate. *Nature* **1987**, *326*, 655− 661.

(46) Draxler, R. R.; Rolph, G. D. HYSPLIT (HYbrid Single-Particle Lagrangian Integrated Trajectory) Model access via NOAA ARL READY Website (http://www.arl.noaa.gov/ready/hysplit4.html); NOAA Air Resources Laboratory: Silver Spring, MD, 2003.